The onset of interfacial waves in the Terahertz spectrum of a nanoparticle suspension

Alessio De Francesco,[1,2] Luisa Scaccia,[3] Ferdinando Formisano,[1,2] Eleonora Guarini,[4] Ubaldo Bafile,[5] Marco Maccarini,[6] Ahmet Alatas,[7] Yong Q. Cai,[8] Dmytro Nykypanchuk,[9] and Alessandro Cunsolo[8]

[1] *Consiglio Nazionale delle Ricerche, Istituto Officina dei Materiali, Operative Group in Grenoble (OGG) F-38042, France*
[2] *Institut Laue-Langevin (ILL), F-38042 Grenoble, France*
[3] *Dipartimento di Economia e Diritto, Università di Macerata, Via Crescimbeni 20, 62100 Macerata, Italy*
[4] *Dipartimento di Fisica e Astronomia, Università di Firenze, via G. Sansone 1, I-50019 Sesto Fiorentino, Italy*
[5] *Consiglio Nazionale delle Ricerche, Istituto di Fisica Applicata "Nello Carrara", via Madonna del Piano 10, I-50019 Sesto Fiorentino, Italy*
[6] *Université Grenoble-Alpes, Grenoble INP, TIMC-IMAG, 38000 Grenoble, France*
[7] *Argonne National Laboratory, Advanced Photon Source, P.O. Box 5000 Upton, NY, 11973, USA*
[8] *Brookhaven National Laboratory-National Synchrotron Light Source-NSLS II, P.O. Box 5000 Upton, NY, 11973, USA*
[9] *Center for Functional Nanomaterials, Brookhaven National Laboratory, Upton, New York 11973, USA*

(Dated: January 28, 2025)

We used Inelastic X-ray Scattering to gain insight into the complex Terahertz dynamics of a diluted Au-nanoparticles suspension in glycerol. We observe that, albeit sparse, Au-nanoparticles leave clear signatures on the dynamic response of the system, the main one being an additional mode propagating at the nanoparticle-glycerol interface. A Bayesian inferential analysis of the lineshape reveals that such a mode, at variance with conventional acoustic modes, keeps a hydrodynamic-like behavior well beyond the continuous limit and down to sub-nanometer distances.

Understanding acoustic propagation through inhomogeneous media is of formidable scientific relevance in many areas, including medical ultrasonography, seismology, vibration noise reduction, and non-destructive testing. From a fundamental perspective, what makes this topic especially compelling is the wide variety of phenomena happening over distances comparable or shorter than some heterogeneity size, l, such as an interlayer spacing, a cluster width or a nanoparticle diameter. In a scattering experiment, the presence of a homogeneity breach might emerge whenever the exchanged wavevector Q matches $2\pi/l$. Under this condition, this broken symmetry possibly results in the onset of multiple spectral modes [1]. Colloidal suspensions in liquids are among the simplest prototypes of heterogeneous materials exhibiting a multiple excitation behavior, as suggested by Brillouin Light Scattering (BLS) measurements [2–6].

Although dynamic studies on liquid suspensions are well documented in the literature, they seldom cover the mesoscopic regime probed by Inelastic X-Ray (IXS) and Neutron Scattering. In this extremely high-Q window, the inequality $Qd_c \gg 1$ (with d_c being the colloid diameter) holds validity even for nanometer-sized colloids, and acoustic propagation is dominated by multiple scattering. Indeed, reflections of acoustic waves at the colloid interface become more likely and prevent sound waves in the liquid from leaking into the colloid, and vice-versa. Consequently, this high Q regime is characterized by the coexistence of acoustic modes selectively propagating either through the solid, or through the liquid, or at their interface. The latter modes are customarily referred to as Stoneley waves [7], and their presence in colloidal suspensions was documented by BLS measurements [2, 4]. In addition, owing to multiple reflections, acoustic waves acquire substantial mutual dephasing, and their interference thus drastically enhances acoustic damping. Interestingly, both effects mentioned above have been observed in a recent IXS study on an aqueous suspension of Au-nanoparticles (Au-Np) [8] and partially in Ref. [9].

This study proves that the immersion of even a sparse amount of NP in a fluid can significantly affect the terahertz acoustic propagation. Even though preliminary, this important result revitalize the intent of controlling the terahertz acoustic properties of a medium upon structural modifications at a mesoscopic scale. Shedding further light onto this fascinating topic is one of the strongest motivations of this work.

Given these grounds, we measured the IXS spectrum of diluted suspensions of Au-nanospheres in glycerol using a well-assessed Bayesian analysis which enabled the determination of the number and shape of excitations contributing to it [10]. The volume concentration was about 0.5%, and d_c equal to either 50 nm or 200 nm. These IXS measurements were jointly analysed with previous IXS data on pure glycerol at 660 bar and ambient temperature [11].

Measurements were executed using the Sector 30 beamline [12, 13] of the Advanced Photon Source (APS) at Argonne National Laboratory. The instrument was operated using the ≈ 23.7 keV harmonic of the undulator source, which corresponds to the Si(12 12 12) backscattering reflection from both the monochromator and energy analyzers. Spectral acquisitions covered the $3 \div 21$ nm^{-1} Q-range with a 2 nm^{-1} Q step. The instrumental resolution function was measured through the IXS signal from a Plexiglas sample at the Q of its first sharp

diffraction maximum, i.e. about 10 nm^{-1}. The resulting spectrum had a 0.8 meV broad (half width at half maximum, HWHM) nearly Lorentzian profile, sufficient to properly resolve the relevant spectral features discussed in the remainder of this paper.

Citrate-capped Au-Np highly monodisperse in both size and shape were purchased by Nanopartz and then immersed in a matrix of 99.9% pure glycerol. According to the manufacturer specifications, the size variance is less than 2 %. The suspensions were embedded in 10 μm thick quartz capillaries having 1 mm outer diameter and wax-sealed on the top. The electronic noise background and empty cell scattering were found to yield a negligible contribution to the measured signal.

Although the Au-Np are sparse, the dynamic response of the suspensions differs significantly from that of pure glycerol, as clearly shown in Fig. 1. There the spectral shapes measured on the 200 nm Au-Np suspension at some representative Q's are compared with pure glycerol spectra; the latter spectra were collected in previous IXS measurements [11] carried out with the same spectrometer setup, yet on a sample at a higher pressure (660 bar). Spectra from the 50 nm diameter particles are instead reported in Fig. S1 of the Supplemental Material (SM) of this paper [14]. In Fig. 1 all curves are normalized to the respective maxima and vertically offset for clarity; furthermore, the resolution profile pertinent to the $Q = 3$ nm^{-1} spectrum is also reported for reference after similar normalization.

A few qualitative trends readily emerge even from a quick inspection of the plotted lineshapes. First, at the lowest Q's the inelastic portion of the pure glycerol spectrum is dominated by broad side shoulders arising from generalized acoustic modes, whose relative amplitude seems greatly depressed upon Au-Np immersion, consistently with what reported in our previous IXS work on an aqueous Au-Np suspension [8]. Also, upon increasing Q, these side shoulders rapidly broaden and lose intensity to the extent of becoming essentially indistinguishable from the spectral background. Most importantly, let's point the attention on the Au-Np suspension spectra which have a central peak significantly broader than their pure glycerol counterparts; below we will discuss this aspect in further depth.

To shed some light on this difference, we performed a lineshape modeling of the measured spectra, in which the IXS intensity was approximated as:

$$I(Q,E) = S(Q,E) \otimes R(Q,E) + B(E), \qquad (1)$$

where $E = \hbar\omega$ is the energy transferred from the probe particle to the target sample. Here, the symbol "$\otimes$" denotes the convolution operator, while $R(Q,E)$ and $B(E)$ are the instrumental resolution function and an usually mildly (linearly) energy-dependent spectral background. In Eq. (1), $S(Q,E)$ is the dynamic structure factor that

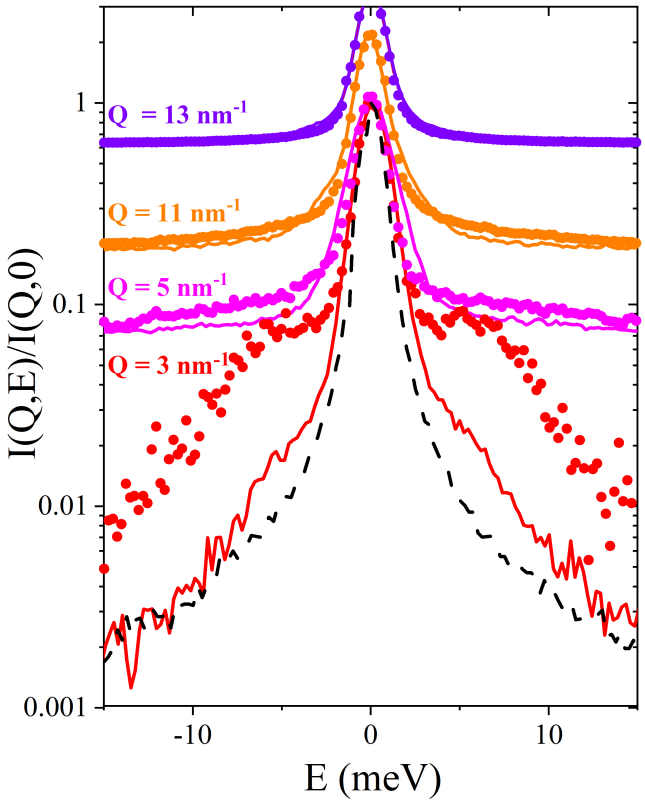

FIG. 1. Representative IXS spectra of the (200 nm sized) Au-Np suspension (solid lines) are compared with their glycerol counterparts (dots). Each suspension spectrum was collected at the Q value indicated, while the corresponding of pure glycerol were measured at Q values higher by 0.5 nm^{-1}. The lowest Q spectra are also compared with the energy resolution function after a similar normalization (red dashed curve). For the sake of comparison, all lineshapes are normalized to their maxima, and are vertically offset for clarity.

can be written as $S(Q,E) = K(E)S_{sym}(Q,E)$ by introducing the energy-dependent detailed balance coefficient $K(E) = (E/k_BT)[n(E)+1]$, with T and k_B being the temperature and the Boltzmann constant, respectively. This term accounts for the statistical population of the generic E-state via the Bose statistics factor $n(E) = (e^{E/k_BT}-1)^{-1}$ and produces the correctly asymmetric spectral shape. Finally in Eq. (1) we assumed:

$$S_{sym}(Q,E) = A_e(Q)\delta(E) + L_{A_0,z_0}(Q,E) + \sum_{j=1}^{k} A_j(Q)DHO_j(Q,E), \qquad (2)$$

where $\delta(E)$ is the Dirac delta function accounting for the elastic peak in the spectrum having amplitude $A_e(Q)$ and accounting for all dynamic processes in the sample which are too slow to be resolved by the measurement;

the other terms are a quasielastic Lorentzian contribution $L_{A_0,z_0}(Q,E)$ having width $z_0(Q)$ (HWHM) and amplitude $A_0(Q)$, and k inelastic contributions modeled as Damped Harmonic Oscillators with amplitudes $A_j(Q)$, written as:

$$DHO_j(Q,E) = \frac{2}{\pi}\frac{\Omega_j^2(Q)\Gamma_j(Q)}{(E^2-\Omega_j^2(Q))^2+4[E\Gamma_j(Q)]^2} \quad (3)$$

where $\Omega_j(Q)$ and $\Gamma_j(Q)$ are the undamped energies and the damping coefficients of the DHO excitations. Notice that the number k of $DHO_j(Q,E)$ excitations likely to appear in the spectrum and their shape coefficients are equally treated as adjustable parameters. Finally, a Lorentzian contribution is needed to account for a possible quasielastic contributions due to a structural relaxation, in analogy to what already done in water [8, 15, 16].

Best fitting values of the model lineshape where determined using a Bayesian inferential analysis implemented through a Markov chain Monte Carlo (MCMC) routine with reversible jump (RJ) steps. This approach can be used to probabilistically infer the joint posterior probability distribution of model parameters, which conveys important information about uncertainties of best-fitting results. Of course, the knowledge of the entire posterior distribution of each parameter also enables one to identify the best-fitting value of such a parameter with the mode of its posterior, whenever the latter, albeit not necessarily symmetric, is sharply peaked, well-shaped and unimodal. The various aspects of this Bayesian analysis are discussed in great detail in Ref. [10] and [17].

The best-fit analysis described above delivered $k = 1$ or 2 depending on the Q value. Fig. 2 compares IXS spectra measured in pure glycerol and in the 200 nm Au-Np suspension at a few representative Q values with the respective best-fitting lineshapes and the individual spectral components introduced in Eqs. (2) and (3); equivalent curves for the 50 nm Au-Np suspension are shown in Fig. 2S of the Supplemental Material. Again, the IXS spectral shapes of glycerol are those previously measured in Ref. [11].

Overall, both Figs. 1 and 2 evidence that the high-frequency inelastic modes in glycerol spectra persist in the Np suspension ones, yet with a strongly reduced relative amplitude.

The comparison in Fig. 2 of experimental and model lineshapes in the two samples, further stresses the emergence of an additional low-frequency mode in the Au-Np suspension spectrum whose origin is still mostly unclear but whose effect is to produce the broadening of the central peak mentioned before. A more precise assignment of this low-energy mode, hereafter referred to as DHO_1, can be gained from Fig. 3 where the best-fit values of its inelastic shift (Ω_1) is compared to the one (Ω_2) of the high-energy mode, DHO_2. Current results are therein compared with previous IXS data on pure glycerol [18],

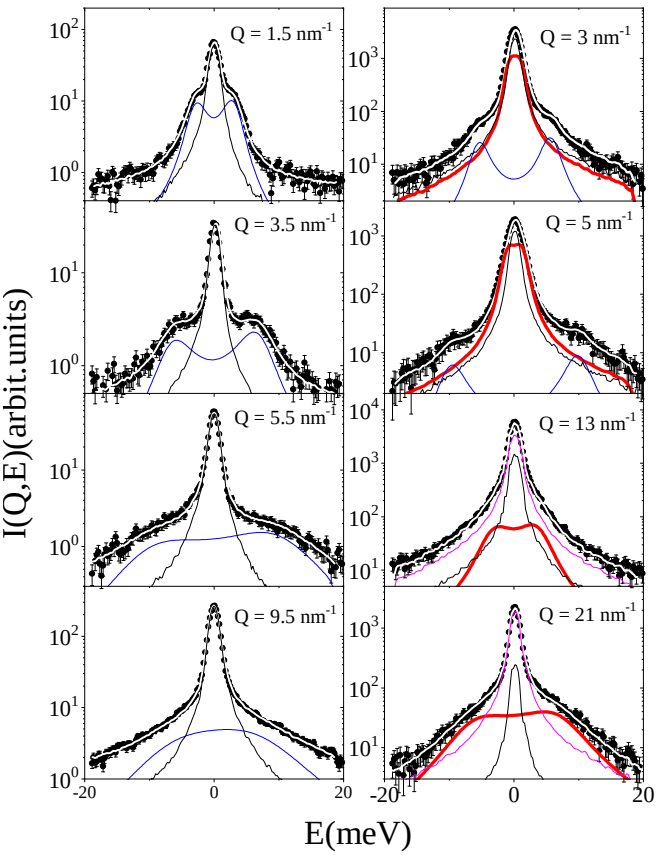

FIG. 2. Panel (a)-(d): representative IXS spectra of pure glycerol measured at some representative Q's (dots) are compared with the best-fitting model lineshapes (white lines) along with its elastic (black line) and the inelastic DHO profile (blue line). Panel (e)-(h): the same as in the left panel but referring to the 200 nm diameter Au-Np suspension in glycerol. Here the thick red and magenta lines represent the additional low frequency excitation and the quasielastic Lorentzian contribution to the spectra, respectively.

and with both the hydrodynamic linear dispersion $\hbar c_s Q$ and its elastic counterpart $\hbar c_\infty Q$, where $c_s = 1920$ m/s and $c_\infty = 3100$ m/s are the adiabatic and the elastic value of the sound velocity in glycerol, respectively derived from Refs. [19] and [20].

Current pure glycerol data displayed in Fig. 3 are obtained from re-analysing, with the discussed Bayesian approach, previous IXS measurements in Ref. [11]. Results on the 50 nm Au-Np suspension are also included for comparison, as measured either in this experiment (see Supplemental Material) or in our previous lower resolution IXS measurements in [8].

Overall, data in Fig. 3 exhibit a few clear trends discussed below in some detail.

a) The high-energy branch

This dispersive branch has been thoroughly investigated in literature and it is commonly assigned to a collective acoustic-like longitudinal excitation of glycerol. At low

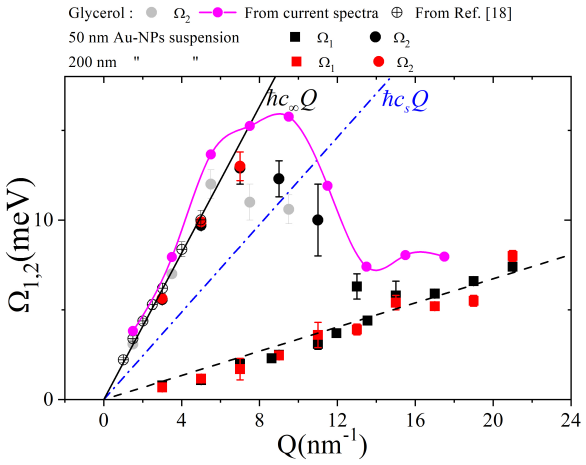

FIG. 3. Fitted values of low (Ω_1) and high (Ω_2) excitation energies are reported as a function of Q, the meaning of various symbols being specified in the legend. The 50nm Ω1 curve (black squares) include also values obtained from the analysis of spectra measured on the Sector 3 beam line of APS in the same experimental conditions of the present experiment, at Q =8.52, 11.95 and 13.55 nm^{-1}. The hydrodynamic linear dispersion of glycerol (blue dash-dotted line) and its "infinite frequency" counterpart (solid black line) having velocities of 1920 m/s and 3100 m/s respectively, are also shown for reference. The dashed black line represents the linear best fit of all Ω_1 values yielding a velocity of 520m/s. Grey dots are obtained by applying the Bayesian analysis to IXS spectra of pure glycerol [11]. The maxima positions of the spectra of the longitudinal current autocorrelations, also derived from Ref. [11] for pure glycerol, are shown as magenta dots+spline. Finally, crossed circles represent the frequency of the DHO peaks obtained by Sette et al. for pure glycerol.

and moderate Q's, the frequency of this mode, Ω_2, largely exceeds the linear hydrodynamic dispersion, closely approaching the elastic one $c_\infty Q$. This owes to the circumstance that in the Q window probed by the current measurement, we prove the elastic response of the system. Also, the comparison between Ω_2's in pure glycerol and in the suspensions suggests that, at this low concentration, immersed Au-Np have little or no influence on the propagation of high-frequency density fluctuations.

At higher Q values, Ω_2 bends downward from the linear law $c_\infty Q$ due to the coupling of sound propagation with first-neighbor molecular ordering. Finally, at even higher Q's, Ω_2 can no longer be determined reliably, due to the gradual disappearance of the DHO$_2$ profile (see, e.g., Fig. 2), for both pure glycerol [18] and for the suspension.

We thus resorted to a different method to achieve an at least approximate determination of the high-frequency dispersive branch. As often proposed for simpler fluids, we estimated it through the maxima positions, Ω, of the function $(E/Q)^2 I(Q,E)$, assumed to be an "experimental" analogue of the spectrum of the longitudinal current autocorrelation $(E/Q)^2 S(Q,E)$. Here, $I(Q,E)$ represents the measured signal after subtraction of the background intensity. Some of these spectra are shown in Fig. S3 of the Supplemental Material, while Ω values estimated for glycerol are included as magenta dots+line in Fig. 3. Similar spectral functions obtained for the 50 nm Au-Np suspension are reported in Fig. S4 of SM. This more extended determination of the dispersion shows a very typical trend, characterized by a bending downwards to a minimum close to the position of the first sharp diffraction maximum, *i.e.* about 14 nm^{-1}. The circumstance that Ω_2 values are consistent for the 50 nm and 200 nm suspensions likely owes to the large Qd_c values considered in these measurements ($Qd_c \geq$ 150 and 600 for the two samples), which make the Au-Np assimilable to huge bodies with infinite radius of curvature, *i.e.* essentially "rigid walls".

b) The low-energy branch

Although evidence for a low-energy, DHO$_1$, profile is found in all IXS spectra from the suspension sample, for $Q \leq 9$ nm^{-1} its two peaks get too close to be adequately resolved by the measurement.

Interestingly, best fit values of Ω_1 exhibit a nearly linear Q-increase across the whole Q range, and bear no evidence for a coupling with the local order, which primarily causes a minimum at the Q-position of the first diffraction peak. The mere existence of an additional low-energy mode in the suspension spectrum is interesting and deserves further comments. Although a second acoustic mode was observed by several quasi-macroscopic measurements on suspensions of silica or plexiglas colloids [2, 5, 21], no evidence was documented at mesoscopic scales. Indeed the only inelastic excitations thus far detected by IXS measurements on suspensions [8] are those either propagating throughout the liquid matrix or confined in the NP interiors.

The linear dispersion of Ω_1 leads to estimate a propagation speed of about (52 $\pm$ 2)10 m/s, i.e. much lower than the sound speeds of both glycerol and gold. This evidence could reveal the physical origin of such a mode, as the only excitation expected to propagate in a composite (liquid-solid) medium with a speed lower than the longitudinal sound velocities in both components is a Stoneley wave [22]. This is a propagating wave whose amplitude decays with increasing distance from the liquid-solid interface. It is worth noticing that the present findings extend previous BLS results [2, 4] into a Q region well beyond the continuum limit and involving distances comparable with first-neighbor molecule separations.

Fig. 4 illustrates the Q-dependence of Γ_1, for the 200 nm and 50 nm Au-Np suspensions. As often the case of IXS lineshape data analyses, the values have sizable scattering, as the determination of line-widths is usually less accurate than, for instance, Ω_1 in Fig.3. However, displayed values look compatible with a Q^2 growth though they cannot rule out other functional forms), as shown by the comparison with parabolic best fits; this suggests

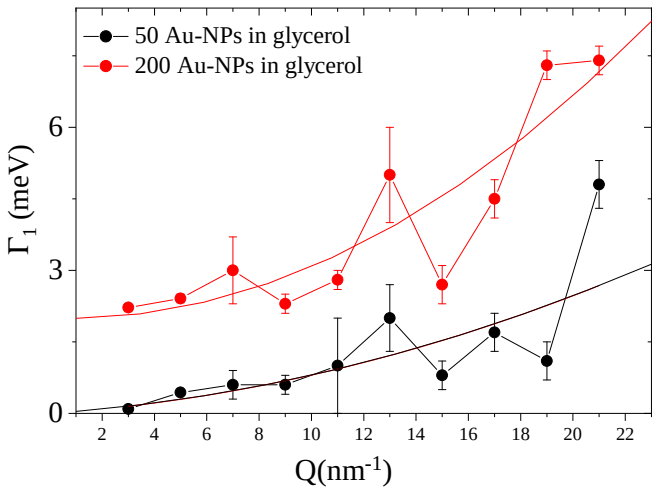

FIG. 4. Best fit values of the low-energy mode halfwidth (Γ_1) for the suspensions of 200 nm (red dots) and 50 nm (black dots) diameter Au-Np are reported as function of Q and compared with the respective parabolic fits (lines of corresponding colors) mainly serving as a guide to the eye

. Results on the 50 nm Au-Np suspension are vertically shifted for clarity.

the persistence of a hydrodynamic-like behavior in a remarkably extended Q-range, as already discussed for Ω_1.

Although best fitting parabolic curves in Fig. 4 are not exactly parallel, we attributed scarce significance to this difference. In fact, large random oscillation of $\Gamma_1(Q)$ data might unpredictably affect their best fitting parabolas, also making the determination of actual Q-dependence uncertain.

As to the Lorentzian term in Eq. 2, its inclusion in the lineshape model rests on the evidence, for $Q \geq 7$ nm^{-1}, of a quasielastic component broader than the resolution profile. Its average unconvoluted HWHM, $z_0 \sim 0.17$ meV, is similar to that observed in two quasielastic neutron scattering measurements on glycerol [23, 24], and also comparable with the one we estimated in the pure glycerol data only at the highest measured $Q = 17.5$ nm^{-1} ($z_0 = 0.20 \pm 0.02$ meV). The reason why, for pure glycerol, this mode emerges at this Q only is still unclear, even though it might owe to the more intense wings of the longitudinal acoustic shoulders partially hiding fine quasielastic features of the spectrum. Also, the observed behaviour is not in contrast wit h the more popular $\delta(E)$ modelling of the central peak of pure glycerol IXS spectra at lower Q's [18, 20, 25].

In conclusion, we discussed here the results of an Inelastic X-Ray Scattering study of the Terahertz spectrum of density fluctuations in a hybrid, liquid-solid, material such as a suspension of Au-nanoparticles in glycerol. A joint Bayesian analysis of the current IXS measurements and previous ones in pure glycerol, unambiguously demonstrates that the presence of an even small concentration of nanoparticles causes the emergence of an additional spectral mode, similar to the one observed by BLS measurements in the hydrodynamic regime, which we assign to Stoneley waves propagating at the NP-glycerol interface. Interestingly, this mode keeps an almost linear dispersive behavior down to mesoscopic scales without displaying Q-oscillations typically relating to local ordering, or any visible interactions with higher energy acoustic mode. Overall, the present study probes the dynamic response of a suspension over distances comparable with nearest neighbor atomic separations, thus ideally complementing previous spectroscopic measurements only covering continuous, or quasi-macroscopic, scales. [2–6]

Additional measurements of NP of various material and shape and dispersed in different liquid matrices will shed further insight into the intriguing spectral behavior discussed in this paper.

This work used resources of the National Synchrotron Light Source II, a U.S. Department of Energy (DOE) Office of Science User Facility operated for the DOE Office of Science by Brookhaven National Laboratory under Contract No. DE-SC0012704.l. This research was also funded by Ente Cassa di Risparmio Firenze (Grant No. 2016-0866) and by Ministero dell'Istruzione dell'Università e della Ricerca Italiano (Grant 591 No. PRIN2017-2017Z55KCW).

[1] P. C. Martin, O. Parodi, and P. S. Pershan, Unified hydrodynamic theory for crystals, liquid crystals, and normal fluids, Phys. Rev. A **6**, 2401 (1972).
[2] J. Liu, L. Ye, D. A. Weitz, and P. Sheng, Novel acoustic excitations in suspensions of hard-sphere colloids, Phys. Rev. Lett. **65**, 2602 (1990).
[3] X. Jing, P. Sheng, and M. Zhou, Theory of acoustic excitations in colloidal suspensions, Phys. Rev. Lett. **66**, 1240 (1991).
[4] L. Ye, J. Liu, P. Sheng, and D. Weitz, Sound propagation in suspensions of solid spheres, Phys. Rev. E **48**, 2805 (1993).
[5] R. Penciu, G. Fytas, E. Economou, W. Steffen, and S. Yannopoulos, Acoustic excitations in suspensions of soft colloids, Phys. Rev. Lett. **85**, 4622 (2000).
[6] R. Penciu, H. Kriegs, G. Petekidis, G. Fytas, and E. Economou, Phonons in colloidal systems, J. Chem. Phys. **118**, 5224 (2003).
[7] R. Stoneley, Elastic waves at the surface of separation of two solids, Proceedings of the Royal Society of London. Series A, Containing Papers of a Mathematical and Physical Character **106**, 416 (1924).
[8] A. De Francesco, L. Scaccia, M. Maccarini, F. Formisano, Y. Zhang, O. Gang, D. Nykypanchuk, A. H. Said, B. M. Leu, A. Alatas, *et al.*, Damping off terahertz sound modes of a liquid upon immersion of nanoparticles, ACS Nano **12**, 8867 (2018).
[9] A. De Francesco, L. Scaccia, F. Formisano, E. Guarini, U. Bafile, M. Maccarini, A. Alatas, Y. C. Cai, and A. Cunsolo, The terahertz dynamics of an aqueous

nanoparticle suspension: An inelastic x-ray scattering study, Nanomaterials **10**, (2020).

[10] A. De Francesco, E. Guarini, U. Bafile, F. Formisano, and L. Scaccia, Bayesian approach to the analysis of neutron Brillouin scattering data on liquid metals, Phys. Rev. E **94**, 023305 (2016).

[11] A. Cunsolo, B. M. Leu, A. H. Said, and Y. Q. Cai, Structural and microscopic relaxations in glycerol: an inelastic x-ray scattering study, J. Chem. Phys. **134**, 184502 (2011).

[12] A. H. Said, H. Sinn, and R. Divan, New developments in fabrication of high-energy-resolution analyzers for inelastic x-ray spectroscopy, J. Synchrotron Radiat. **18**, 492 (2011).

[13] T. Toellner, A. Alatas, and A. Said, Six-reflection mev-monochromator for synchrotron radiation, J. Synchrotron Radiat. **18**, 605 (2011).

[14] See Supplemental Material at [insert url] for IXS spectra of 50nm diameter AuNP's, selected spectra at four different momentum transfer vectors Q with corrispondent best fits and lineshape analysis, experimental current spectra for pure glycerol and 200nm AuNP's suspension in glycerol.

[15] G. Monaco, A. Cunsolo, G. Ruocco, and F. Sette, Viscoelastic behavior of water in the terahertz-frequency range: an inelastic x-ray scattering study, Phys. Rev. E **60**, 5505 (1999).

[16] A. Cunsolo, G. Ruocco, F. Sette, C. Masciovecchio, A. Mermet, G. Monaco, M. Sampoli, and R. Verbeni, Experimental determination of the structural relaxation in liquid water, Phys. Rev. Lett. **82**, 775 (1999).

[17] P. J. Green, Reversible jump markov chain monte carlo computation and bayesian model determination, Biometrika **82**, 711 (1995).

[18] F. Sette, M. H. Krisch, C. Masciovecchio, G. Ruocco, and G. Monaco, Dynamics of glasses and glass-forming liquids studied by inelastic x-ray scattering, Science **280**, 1550 (1998).

[19] M. Rajeswari and A. Raychaudhuri, Specific-heat measurements during cooling through the glass-transition region, Phys. Rev. B **47**, 3036 (1993).

[20] A. Giugni and A. Cunsolo, Structural relaxation in the dynamics of glycerol: a joint visible, uv and x-ray inelastic scattering study, J. Phys.: Condens. Matter **18**, 889 (2006).

[21] X. Jing, P. Sheng, and M. Zhou, Acoustic and electromagnetic quasimodes in dispersed random media, Phys. Rev. A **46**, 6513 (1992).

[22] L. Brekhovskikh, *Waves in layered media*, Vol. 16 (Elsevier, 2012).

[23] D. Aranghel, V. Tripadus, A. Radulescu, M. Petre, M. Dima, and C. Petre, Quasielastic neutron scattering on glycerol, J. Optoelectron. Adv. Mater. **12**, 953 (2010).

[24] A. Vispa, S. Busch, J. L. Tamarit, T. Unruh, F. Fernandez-Alonso, and L. C. Pardo, A robust comparison of dynamical scenarios in a glass-forming liquid, Phys. Chem. Chem. Phys. **18**, 3975 (2016).

[25] G. Monaco and V. Giordano, Breakdown of the debye approximation for the acoustic modes with nanometric wavelengths in glasses, Proc. Natl. Acad. Sci. USA **106**, 3659 (2009).